Available online at www.sciencedirect.com
ScienceDirect
Trans. Nonferrous Met. Soc. China 25(2015) 1961−1967
Transactions of Nonferrous Metals Society of China
www.tnmsc.cn

Development of black Ni−Co alloy films from modified Watts electrolyte and its morphology and structural characteristics

R. SEKAR, K. K. JAGADESH, G. N. K. RAMESH BAPU

Electroplating and Metal Finishing Technology Division, CSIR-Central Electrochemical Research Institute, Karaikudi 630006, Tamil Nadu, India

Received 23 July 2014; accepted 26 November 2014

Abstract: The electrodeposition of black Ni−Co alloy film from Watts nickel solution and the effects of benzotriaozole and imidazole as the additives were studied. The electrolyte consists of $NiSO_4$, $NiCl_2$, H_3BO_3, $CoSO_4$ and KNO_3. The cathode current efficiency and the throwing power of the solution and the film adhesion to the mild steel metallic foil were determined by standard methods. The crystal structure, lattice parameter, crystal orientation and crystal size were analyzed by X-ray diffraction (XRD). Moreover, the surface morphology and elemental composition of the black Ni−Co alloy films were analyzed by scanning electron microscopy (SEM) and energy dispersive X-ray spectroscopy (EDX) techniques. The darkness of the black films increases with increasing the incorporation of Co ion into the films. The XRD studies reveal that the black Ni−Co alloy films exhibit Ni (111) as the preferred orientation.

Key words: additive; electrodeposition; black Ni−Co alloy; adhesion

1 Introduction

Black Ni films have distinctive appearance and are especially suitable for articles like optical, camera fittings, hardware and electrical instruments. Another application of the electrodeposition process is in the manufacture of metal name plates, in which it is used to produce a black finish on the etched background [1]. Black films such as black Co [2,3] and black Ni [4] have performed as more efficient solar collector surfaces. Trivalent black Cr and black Co films have been studied for structural and morphological behavior under the plated and annealed conditions [5]. YOUSIF [6] studied the modification of the electrodeposition method by adding $CuSO_4$ for improving the blackness of the black Mo films for solar energy applications. THARAMANI and MAYANNA [7] studied the electrodeposited black Co−Ni alloy films as a solar selective surface for solar energy applications. The X-ray photoelectron spectroscopy (XPS) and X-ray auger electron spectroscopy (XAES) investigations were carried out on the electrochemically deposited solar selective black Co−Ni alloy films on the Mo substrate [8].

Solar absorber black films have been obtained from several techniques such as sputtering [9], chemical vapour deposition [10], chemical conversion [11], electroless plating [12] and electro plating [13]. In order to achieve the control and reproducibility of the film to qualify as an industrially useful material, the deposition process must be properly selected. The required properties of the metallic film may be better controlled by direct electrodeposition. Black Ni electrodeposits may mainly consist of nickel sulphide and Zn together with free Ni. According to IBRAHIM [14], the deposition of metals from their ammonia complexes is more difficult than from the free metal ions and the reduction of thiocyanate becomes the preferred reaction. The present investigation aims to develop adherent black Ni−Co alloy films from modified Watts nickel solution containing KNO_3. In addition, the effects of benzotriazole and imidazole as the additives are studied in the modified solution to improve the surface morphology and the grain size of the films.

2 Experimental

The electrodeposition of black Ni−Co alloy films

Corresponding author: R. SEKAR; Tel: +91-4565-241572, +91-9940874641; Fax: +91-4565-227779; E-mail: grsek2004@yahoo.com
DOI: 10.1016/S1003-6326(15)63804-3

was performed using a bath containing $NiSO_4·6H_2O$, $NiCl_2·6H_2O$, $CoSO_4·7H_2O$, and H_3BO_3 with various concentrations of KNO_3 (Table 1). All the plating solutions and reagents were made from AR grade chemicals and prepared from double distilled water. Before plating, activated charcoal treatment and dummy electrolysis were carried out to remove the organic and inorganic impurities from the bath. For the electrodeposition, a mild steel panel of 5 cm × 5 cm × 0.1 cm was used as the cathode. Two pure Pt anodes with the same area as the cathode were used on either side of the cathode. The plating cell was a wide-mouthed glass vessel and the electrodes were fixed on each of the side walls. Surface preparation prior to deposition is an important factor and can be achieved by the mechanical and electrochemical methods [15]. The procedure was adopted to remove the surface scales, using acid dipping and mechanical polishing to get a smooth surface, degreasing with trichloroethylene and final electrocleaning at 4 A/dm^2 in a solution consisting of NaOH and Na_2CO_3 (30 g/L for each), then washed with tap water and rinsed with distilled water and ethanol. Direct current was supplied by a DC power supply unit (Aplab DC regulated power supply unit). The plating bath was operated at 30 °C at different current densities. Electrodeposition was carried out for 10 min in each case. The cathodes were weighed before and after deposition and the cathode current efficiency was calculated using Faraday's law. The percentage of the throwing power (TP) of the solution was measured using a Haring−Blum cell [16], consisting of two metallic steel foil cathodes of 7.5 cm × 5 cm × 0.1 cm filling the entire cross section at both ends, and one perforated metallic Ni foil as the anode of the same size. The anode was placed between the cathodes, and the distance from the anode to one of the cathode was one-fifth of that to the other. The values of the throwing power for different solutions used were calculated using Field's formula:

$$\text{Throwing power} = \frac{L-M}{L+M-2}\times 100\% \quad (1)$$

Table 1 Bath composition of various plating solutions

Composition	Concentration/(g·L^{-1})			
	Bath A	Bath B	Bath C	Bath D
$NiSO_4$	211	211	211	211
$NiCl_2$	24	24	24	24
H_3BO_3	31	31	31	31
KNO_3	25	25	25	25
$CoSO_4$	−	20	20	20
Benzotriazole	−	−	0.5	−
Imidazole	−	−	−	0.5

where L is the ratio of the respective distances from the anode to the far and near cathodes, M is the metal distribution ratio between the near and far cathode.

The bend test (ASTM test method B571-84 [17]) was performed to evaluate the adhesion of the black Ni−Co alloy films. The X-ray diffraction patterns were analyzed using an X-pert pro power diffraction system PE 3040/60 for black Ni−Co alloy films produced from different baths in the presence and absence of additives. The samples were scanned in 30°−100° (2θ) at a scan rate of 1 (°)/min using Cu K_α (λ =0.15405 nm) radiation. The peaks due to the different phases were identified and the corresponding lattice parameters were calculated. The crystal size of the black Ni−Co alloy films were calculated using the Scherrer formula [18,19] from the predominant peak.

$$t = \frac{0.9\lambda}{\beta\cos\theta} \quad (2)$$

where t is the average size of the crystallites, 0.9 is the Scherrer constant, λ is the wavelength of the radiation, β is the peak width at half maximum, and θ corresponds to the peak position.

The scanning electron microscopy (SEM) photographs were taken using a TESCAN at 25 kV and the elemental composition was analyzed by energy dispersive X-ray spectroscopy (EDX) using the same instrument. Molecular imaging atomic force microscopy (AFM) was used in a contact mode with a Si_3N_4 tip to reveal the 3D surface topography of the films.

3 Results and discussion

3.1 Cathode current efficiency studies

3.1.1 Effect of KNO_3 on cathode current efficiency

The cathode current efficiency of the pure black Ni film in the absence and presence of 10−35 g/L KNO_3 is shown in Fig. 1 (Bath A). In the absence of KNO_3, the cathode current efficiency is 98%−99%. However, with increasing the amount of KNO_3 in bath A, the cathode current efficiency decreases and reaches 63% at 20 g/L KNO_3, which is steadily maintained thereafter. Hence it is suggested that the cathode current efficiency (CCE) of black Ni electrodeposition depends strongly on the KNO_3 concentration. Further increasing the concentration of KNO_3 above 20 g/L, there is no significant change in the CCE. It is possible that the reduction in the deposition rate with increasing the concentration of KNO_3 could be attributed to its adsorption on the electrode surface which causes a lower rate of electron transfer or nucleation. This effect slows down with further KNO_3 addition as the surface adsorption reaches saturation.

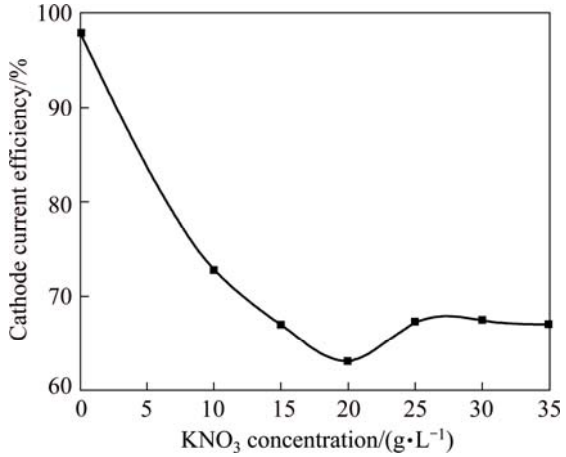

Fig. 1 Variation of current efficiency of black Ni films electrodeposition from bath A with various concentration of KNO_3 at 30 °C and 0.5 A/dm^2

3.1.2 Effect of $CoSO_4$ on cathode current efficiency

The effect of adding $CoSO_4$ for improving the quality of the black Ni film is studied in the modified Watts solution containing 25 g/L KNO_3 in the bath. Figure 2 represents the variation of current efficiency of the black Ni−Co alloy film deposition solution with the addition of $CoSO_4$ ranging in 10−30 g/L (Bath B). The CCE steadily decreases with increasing the concentration of $CoSO_4$. Moreover, when the concentration reaches 20 g/L, the Ni−Co alloy film becomes dark black. Hence, the concentration of 20 g/L $CoSO_4$ is optimum and taken for further studies.

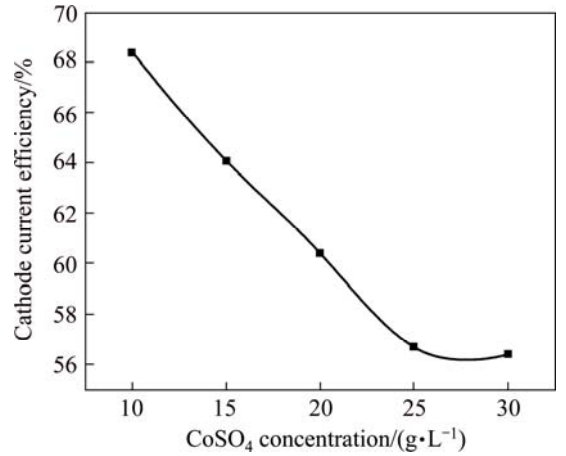

Fig. 2 Variation of current efficiency of black Ni−Co alloy films electrodeposition from bath B with various concentration of $CoSO_4$ at 30 °C and 0.5 A/dm^2

3.1.3 Effect of benzotriazole on cathode current efficiency

Figure 3 represents the variation of current efficiency of black Ni−Co alloy films electrodeposition from bath C containing benzotriazole as the additive (0.25−1.0 g/L). When the concentration reaches 0.5 g/L, the CCE is nearly 62% and then decreases with increasing the concentration of benzotriazole. The CCE obtained from bath C is lower compared with those obtained from baths A and B.

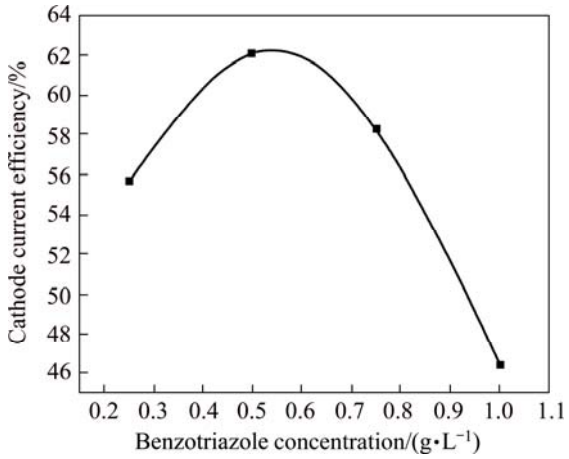

Fig. 3 Variation of current efficiency of black Ni−Co alloy films electrodeposition from bath C with various concentration of benzotriazole at 30 °C and 0.5 A/dm^2

3.1.4 Effect of imidazole on cathode current efficiency

Figure 4 represents the variation of CCE of Ni−Co alloy films electrodepostion from bath D containing imidazole (0.25−1.0 g/L) as the additive. The CCE decreases from 51% to 37% with increasing the imidazole concentration. However, the deposits are jet black as compared with the deposits produced from the additive-free baths.

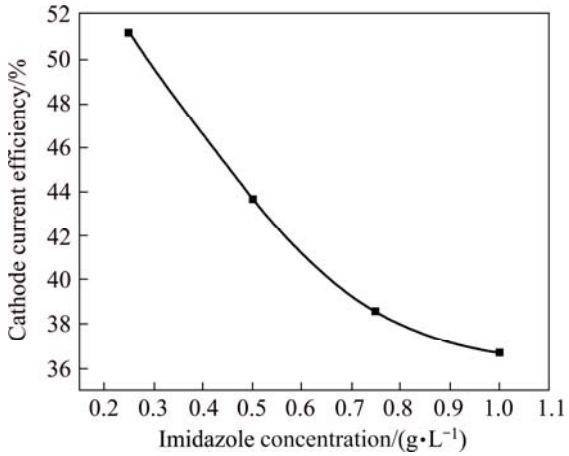

Fig. 4 Variation of current efficiency of black Ni−Co alloy films electrodeposition from bath D with various concentration of imidazole at 30 °C and 0.5 A/dm^2

3.2 Adhesion

The adhesion of the pure black Ni and black Ni−Co alloy films obtained in the presence and absence of additives was tested by subjecting the deposited specimens to the standard bend tests. No flaking or peeling of the deposit was seen on bending. The deposits

from all four baths were found to withstand the bend test, showing that the keying and adhesion of the films to the base were very good in all cases.

3.3 Throwing power

Figure 5 gives the variation of throwing power of baths A, B, C and D at different current densities ranging from 0.5−1.5 A/dm^2. The throwing power of bath A (Fig. 5) increases with increasing the current density, which may be attributed to the increase of the cathodic polarization. With the addition of 20 g/L $CoSO_4$ in bath B (Fig. 5), the throwing power increases with increasing the current densities. Similar increase of the throwing power was observed with increasing the current densities of bath C (0.5 g/L benzotriazole) and bath D (0.5 g/L imidazole). It can be observed that the throwing power of bath D is the highest as compared with that of other baths A, B and C.

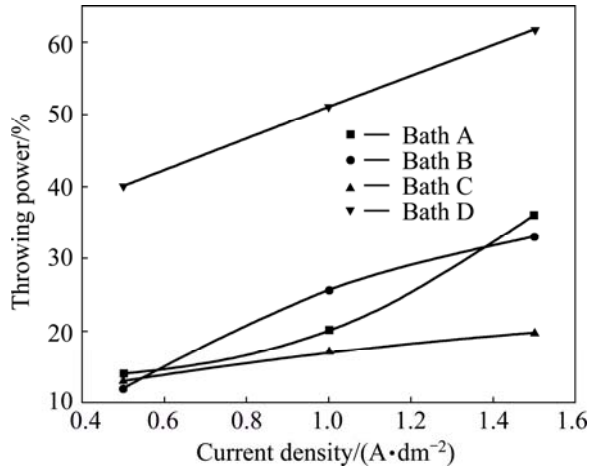

Fig. 5 Variation of throwing power of different baths with various current densities at 30 °C

3.4 X-ray diffraction analysis

The X-ray diffraction patterns of the electrodeposited black Ni and black Ni−Co alloy films on mild steel substrate obtained from various baths are shown in Fig. 6. It is observed from Fig. 6(a) that the film obtained from bath A exhibits polycrystalline nature with face centered cubic (FCC) structure with preferential orientation along FCC (111) plane. This particular black Ni film shows three peaks at 2θ values of 45.00°, 65.33° and 82.58° corresponding to the reflections of the (111), (200) and (220) planes, respectively. The observed 'd' values are in good agreement with the standard values of Ni [20]. The XRD data for black Ni−Co alloy film produced from bath B containing 20 g/L $CoSO_4$ (Fig. 6(b)) shows that with the incorporation of Co into the black Ni−Co alloy film, the intensity of the (111) peak increases and the peak width is broader, which indicates the decrease in the grain size of the black Ni−Co alloy film. The film can be identified as Ni solid solution with a FCC structure. These results confirm that the black Ni film is in fact obtained directly after Ni(II) ion reduction from an aqueous electrolyte containing little amounts of NO_3^-, and this black film is composed of dispersed metallic Ni. Similarly, the color of the deposit becomes darker as compared with the film obtained from Co-free bath. The XRD pattern of the black Ni−Co alloy film (Fig. 6(c)) prepared from bath C containing benzotriazole exhibits (111) peak with strong reflection, and the crystal size decreases significantly in comparison with that of the deposit obtained from the additive free baths A and B (Table 2). The content of Co further increases in the black Ni−Co alloy film and the crystal size is still reduced. Thus it can be seen that benzotriazole reduces the grain size and has a significant effect on the preferred orientation of the deposit, thereby producing the smooth dark black deposits of Ni−Co alloy. Similarly, in Fig. 6(d), the pattern of electrodeposited black Ni−Co alloy film obtained from bath D containing imidazole as the additive shows (111) plane as the preferred orientation and the crystal size of the deposit is significantly reduced (18.36 nm) (Table 2). Generally, the content of Co increases with decreasing the grain size of the film, and the peak width is broader for the film with higher Co content. Hence imidazole shows to be the best grain refiner.

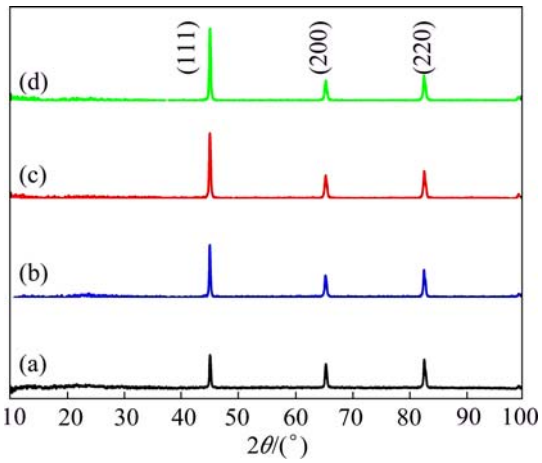

Fig. 6 XRD patterns of black Ni and Ni−Co alloy films obtained from various baths at 30 °C and 0.5 A/dm^2: (a) Bath A; (b) Bath B; (c) Bath C; (d) Bath D

Table 2 Crystal size of black films obtained from various plating solutions at current density of 0.5 A/dm^2

Bath	2θ value/(°)	FWHM value	(*hkl*)	Crystal size/nm
A	45.0563	0.2509	(111)	34.3
B	44.9895	0.3513	(111)	24.5
C	44.6461	0.4015	(111)	21.41
D	44.7598	0.4684	(111)	18.36

3.5 Microstructure analysis

Figure 7 shows the microstructures of black Ni and black Ni−Co alloy films on mild steel metallic foil electrodeposited from various baths. The SEM image of black Ni deposit (Fig. 7(a)) obtained from bath A exhibits an island-like surface morphology with a cracked pattern, which is the characteristics of the inclusion of oxidation product in the coatings and responsible for the black color of the deposit.

Figure 7(b) shows the surface morphology of black Ni−Co alloy produced from bath B containing 20 g/L $CoSO_4$. It reveals that $CoSO_4$ has no significant effect on the morphology but the width of the cracks decreases with increasing the number of the cracks in the coating. Moreover, the deposit becomes darker as compared with the $CoSO_4$-free deposit. Hence it is suggested that the incorporation of Co ion is also responsible for the blackening of the Ni deposit and enhances the oxidation reaction. The incorporation of Co was confirmed by EDX analysis (Table 3). Figure 7(c) shows the SEM micrograph of black Ni−Co alloy obtained from bath C with the addition of benzotriazole (0.5 g/L). It shows that the surface morphology is slightly changed. The increase of the crack pattern shows the inclusion of oxidation products in the coatings, but the incorporation of Co slightly increases (Table 3). Hence it is suggested that benzotriazole not only acts as an antioxidant but also acts as an inhibitor. The SEM micrograph of black Ni−Co deposit from bath D containing imidazole (0.5 g/L) as the additive is shown in Fig. 7(d). The surface morphology of the coating is changed to rather smooth and flat with porous structure. This porous structure enhances the absorbance of the coatings and makes these layers suitable for solar absorber application.

Table 3 EDX data of black films obtained from various plating solutions

Bath	Mass fraction/%				
	Ni	Fe	O	N	Co
A	22.68	22.56	45.99	7.06	−
B	20.99	21.41	42.31	12.55	2.62
C	20.63	23.62	43.85	9.68	2.84
D	17.08	24.78	41.66	12.62	3.67

3.6 EDX analysis

The EDX compositional analysis of black Ni and black Ni−Co alloy electrodeposited on mild steel metallic foil from various electrolytes was made and their elemental composition data are recorded in Table 3. It is observed that the Ni coating obtained from bath A without Co mainly consists of Ni and Ni oxides. From the electrochemical deposition point of view, it is expected that two forms of oxides/hydroxides form in the deposit during the electrolytic deposition. The main incorporation mechanism of the oxide/hydroxide in deposit is through Ni hydroxide precipitation. Ni forms more insoluble hydroxide than Co and it is more likely to be $Ni(OH)_2$ incorporation. Some of the Fe, O and N signals are from the mild steel metallic foil and the oxidizing compound used in the electrolyte.

It can be seen from Table 3 that the Ni−Co deposit obtained from bath B, and the coating mainly consists of Ni, Ni oxide and 2.62% Co (mass fraction). The deposits become darker than that produced from Co-free bath. Hence it is suggested that the incorporation of Co increases the black color of the coatings. So Co ion is also essential for obtaining black coatings.

From Table 3, it is noticed that the black Ni−Co

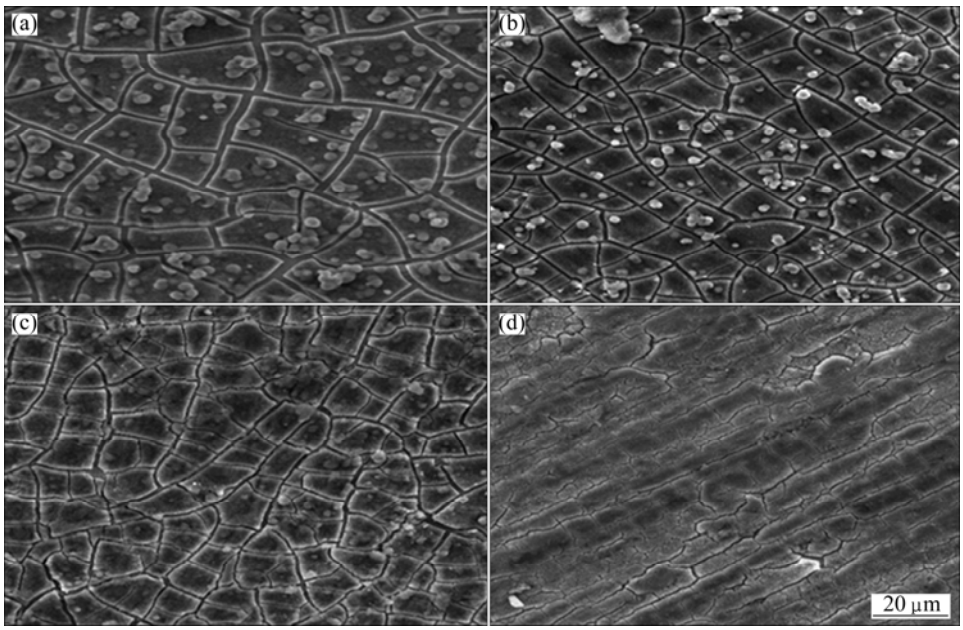

Fig. 7 SEM micrographs of black films obtained from various baths at 30 °C and 0.5 A/dm^2: (a) Bath A; (b) Bath B; (c) Bath C; (d) Bath D

alloy deposit produced from bath C has slightly higher Co incorporation (2.84%, mass fraction) as compared with that of the deposits obtained from bath B. Hence the additive hinders the deposition rate and improves the surface morphology of the coating.

Table 3 also shows that in the deposit prepared from bath D, the percentage of Ni ion decreases and that of Co ion increases (3.67%, mass fraciton) by the addition of imidazole as the additive. Hence the deposit is darker as compared with that obtained from other baths. In general, additives may get adsorbed at the electrode surface thereby blocking the electrode surface and hindering the growing nuclei.

3.7 AFM measurements

Atomic force microscopy (AFM) furnishes more surface structural information than SEM, and the technique delivered mainly to verify the conclusions from the SEM micrographs. The surface topography of the films depends on the pretreatment of the substrate, as well as the chemical composition and deposition conditions of the films [21]. The AFM imaging gives a perspective of "Z" direction with three dimensional images [22]. Figure 8 shows the two-dimensional and three-dimensional AFM images of the films prepared from various electrolytes. Figure 8(a), the representative AFM image scanned over an area of 5 μm × 5 μm, indicates that the film obtained from bath A shows the black Ni film alone exhibiting "rounded-top" morphology with a surface roughness of 16.9 nm. Figure 8(b) shows the films obtained from bath B (black Ni−Co alloy), in which the surface is found to be nearly uniform with a rough surface and pores, and there is no small change in the surface roughness and grain size in the deposit. Moreover, the film is darker than the pure Ni. Figures 8(c) and (d) show the AFM images of the films obtained from baths C and D containing benzotriazole and imidazole additives, respectively, and the AFM images show homogeneous topography with low dispersion in height. It is found that the content of Co increases with increasing the darkness of the films and reduction in the grain size. These results confirm that the additives act as grain refiners with imidazole being the best grain refiner.

4 Conclusion

1) Smooth and adherent black Ni and black Ni−Co alloy films were obtained from Watts based electrolytes with moderate current efficiency and good throwing power.

2) The characteristic XRD patterns of black Ni and black Ni−Co alloy with different orientation of lattice planes were observed, and the (111) plane is more predominant for the films obtained from all the baths. The crystal size calculation based on the XRD data reveals that the film obtained from the bath with imidazole as the additive has the smallest crystal size.

3) The SEM micrographs show that the films obtained from bath A and B exhibit island-like structure and crack in nature. The film obtained from bath C shows more cracks and lower incorporation of oxidation product. However, the film obtained from bath D reveals that the film is compact with less cracks and no oxidation products. The EDX analysis reveals that the maximum incorporation of Co in bath D is 3.67%.

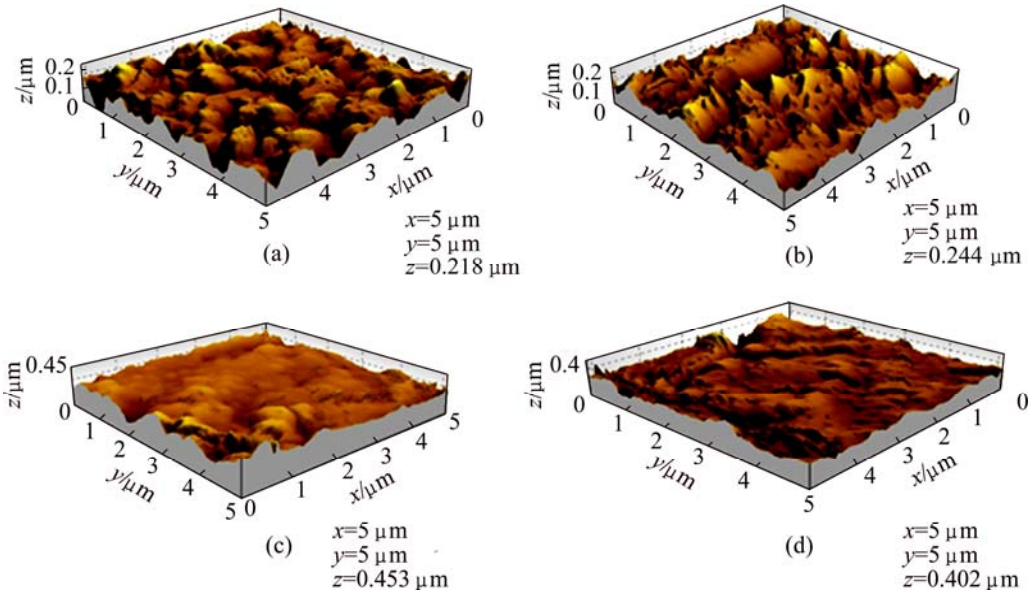

Fig. 8 AFM images for black films obtained from various baths at 30 °C and 0.5 A/dm^2: (a) Bath A; (b) Bath B; (c) Bath C; (d) Bath D

4) The AFM analysis reveals the surface topography of the films, and the study of the grain refinement brought about by the additives shows that imidazole is the best grain refiner.

References

[1] ESSEX F J, PROBERT D. The canning handbook of surface finishing and technology [M]. New York: E & F.N. Spon Ltd., 1985: 402.

[2] BARRERA E, PARDAVE M P, BATINA N, GONZALEZ I. Formation mechanisms and characterization of black and white cobalt electrodeposition onto stainless steel [J]. J Electrochem Soc, 2000, 147: 1787−1796.

[3] JOHN S, NAGARANI N, RAJENDRAN S. Black cobalt solar absorber coatings [J]. Sol Energy Mat Sol C, 1991, 22: 293−302.

[4] JOHN S. Electrodeposition of nickel black solar absorber coatings [J]. Met Finish, 1997, 95: 84−86.

[5] JEEVA P A, KARTHIKEYAN S, NARAYANAN S. Performance characteristics of corrosion resistant black coatings [J]. Procedia Engineering, 2013, 64: 491−496.

[6] YOUSIF K M. Modification of the electrodeposition method of molybdenum black coatings for solar energy applications [J]. Met Finish, 1995, 93: 90−94.

[7] THARAMANI C N, MAYANNA S M. Low cost black Cu−Ni alloy coatings for solar selective applications [J]. Sol Energy Mat Sol C, 2007, 91: 664−669.

[8] ARAVINDA C L, MAYANNA S M, BERA P, JAYARAM V, SHARMA A K. XPS and XAES investigations of electrochemically deposited Cu−Ni solar selected black coatings on molybdenum substrate [J]. J Mater Lett, 2002, 21: 205−208.

[9] FAROOQ M, GREEN A A, HUTCHINS M G. High performance sputtered Ni:SiO_2 composite solar absorber surfaces [J]. Sol Energy Mat Sol C, 1998, 54: 67−73.

[10] GAMPP R, OELHAFEN P, GANTENBEIN P, BRUNOLD S, FREI U. Accelerated aging tests of chromium containing amorphous hydrogenated carbon coatings for solar collectors [J]. Sol Energy Mat Sol C, 1998, 54: 369−377.

[11] GESHEVA K A, GOGOVA D S, STOYANOV G. Black tungsten selective optical coatings for photothermal solar energy conversion [J]. J Phys III, 1992, 2(8): 1453−1459.

[12] JOHN S, SHANMUGAM N V, SRINIVASAN K N, SELVAM M, SHENOI B A. Blackening of electroless nickel deposits for solar energy applications [J]. Surf Tech, 1983, 20: 331−338.

[13] IBRAHIM M A M. Black nickel electrodeposition from a modified Watts bath [J]. J Appl Electrochem, 2006, 36: 295−301.

[14] IBRAHIM M A M. Copper electrodeposition from non-polluting aqueous ammonia baths [J]. Plat Surf Finish, 2000, 87: 67−72.

[15] SEKAR R, JAYAKRISHNAN S. Electrodeposition of zinc from acetate baths [J]. Plat Surf Finish, 2005, 92: 58−68.

[16] HAMID Z A. Improving the throwing power of nickel electroplating baths [J]. Mater Chem Phys, 1998, 53: 235−238.

[17] ASTM Test method B571-84. Adhesion of metallic coatings [S]. 02.05 ASTM International.

[18] CULLITY B D. Elements of X-ray diffraction [M]. USA: Addison Wesley Publishing Co Inc, 1967.

[19] KLUG H P, ALEXANDER L. X-ray diffraction procedures for polycrystalline and amorphous materials [M]. New York: Wiley, 1980.

[20] Joint Committee on Powder Diffraction Standards (JCPDS). International Centre for Diffraction File PDF-2 Database Sets-149 [M]. Pennsylvania, 2000.

[21] YOUSIF K M, SMITH B E, JEYNES C. Investigation of microstructure of molybdenum–copper black electrodeposited coatings with reference to solar selectivity [J]. J Mater Sci, 1996, 31: 185−191.

[22] MARTYAK N M, SEEFELDT R. Additive-effects during plating in acid tin methane sulfonate electrolytes [J]. Electrochim Acta, 2004, 49: 4303−4311.

黑色 Ni−Co 合金薄膜的制备及其形貌和结构特征

R. SEKAR, K. K. JAGADESH, G. N. K. RAMESH BAPU

Electroplating and Metal Finishing Technology Division, CSIR-Central Electrochemical Research Institute, Karaikudi 630006, Tamil Nadu, India

摘　要：研究在 Watts 镍溶液中电沉积制备黑色 Ni−Co 合金薄膜以及苯并三唑和咪唑作为添加剂对电沉积薄膜的影响。电解液由 $NiSO_4$、$NiCl_2$、H_3BO_3、$CoSO_4$ 和 KNO_3 组成。用标准方法测试溶液的阴极电流效率和均镀能力以及薄膜在低碳钢基底上的粘附性。通过 X 射线衍射(XRD)研究晶体结构、晶格参数、晶体取向以及晶体尺寸。通过扫描电镜(SEM)和能谱(EDX)分析黑色 Ni−Co 合金薄膜的表面形貌和元素组成。黑色薄膜的颜色随着薄膜中 Co 离子掺入量的增加而加深。XRD 研究表明黑色 Ni−Co 合金薄膜以 Ni(111)面择优生长。

关键词：添加剂；电沉积；黑色 Ni−Co 合金；粘附

(Edited by Mu-lan QIN)